REPORT No. 732

PRESSURE DISTRIBUTION OVER AN NACA 23012 AIRFOIL WITH A FIXED SLOT AND A SLOTTED FLAP

By THOMAS A. HARRIS and JOHN G. LOWRY

SUMMARY

A pressure-distribution investigation was conducted in the LMAL 7- by 10-foot wind tunnel to determine the air loads on an NACA 23012 airfoil in combination with a fixed leading-edge slot and a slotted flap. Pressures were measured over the upper and lower surfaces of the component parts of the combination for several angles of attack and at several flap settings.

The data, presented as pressure diagrams and graphs of section coefficients, are applicable to rib, slat, and flap designs for the combination. The data showed the following: The peak pressures at the nose of the slat and the loads on the slat were higher in the angle-of-attack range where slots are useful than the peak pressures and the loads shown in previously published data on the Handley Page type of slot. The loads on the slotted flap showed only a slight change with the addition of a leading-edge slot, and it is believed that any conventional flap would show only a slight change in loading if incorporated with a fixed leading-edge slot.

INTRODUCTION

The National Advisory Committee for Aeronautics has undertaken an extensive investigation of air loads on high-lift and stall-prevention devices to obtain data useful in the design of safer airplanes. With the increase in wing loading and the use of highly tapered wings, some device is necessary to improve the stalling characteristics of the wing. There are several ways in which these undesirable characteristics can be improved. One method now being employed is the addition of a leading-edge slot to the tip section of the wing.

The simplest leading-edge slot to construct and operate is the fixed slot described in reference 1; in this case the slat is an integral part of the wing. This type of slot has the disadvantage of increasing the drag at the high-speed condition but may be advantageous where ruggedness and simplicity of construction are essential.

Two types of movable leading-edge slot are the Handley Page (reference 2) and the Maxwell (reference 3), which are formed by the movement or rotation of the slat with respect to the main airfoil. Some load data are available on the Handley Page type of slot (references 2 and 4). This type of slot is advantageous because it produces little increase in drag at high-speed conditions and is more effective than the fixed slot, but its construction and operation offer difficulties.

The present investigation includes load data for the optimum fixed-slot arrangement reported in reference 1 and for a slotted flap on an NACA 23012 airfoil.

APPARATUS AND TESTS

MODELS

The airfoil model used in these tests had a 7-foot span and a 3-foot chord; it conformed to the NACA 23012 airfoil profile (table I) and was constructed of laminated mahogany with a hollow section to accommodate the copper pressure tubes. The basic model consisted of the airfoil in combination with a full-span

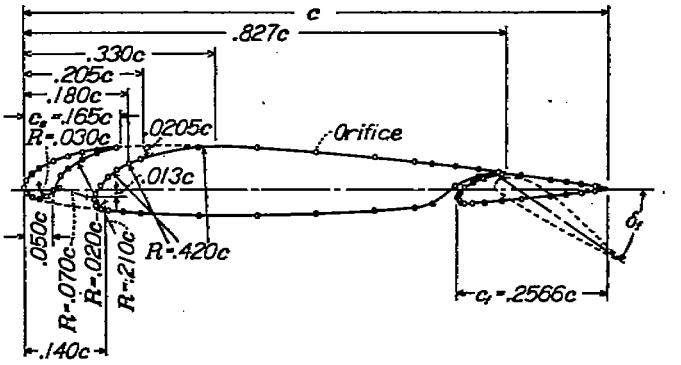

FIGURE 1.—Cross section of model showing airfoil-slot-flap combination used in pressure-distribution tests.

fixed leading-edge slot and a full-span slotted flap (fig. 1). The fixed slat was attached to the airfoil by four thin metal fittings and the slotted flap was attached to the airfoil with three metal hinges.

The full-span leading-edge slot (fig. 1) was developed by the NACA and is designated nose 11, slat 5C in reference 1. The slat has a chord of 5.940 inches (16.50 percent of the over-all airfoil chord). The trailing-edge portion of the slat was constructed of aluminum so that it maintains its shape under load.

The full-span slotted flap (table I) was developed by the NACA and is designated 2–h in reference 5. It has a chord of 9.238 inches (25.66 percent of the over-all airfoil chord). The path of the flap nose (table I) is the optimum one reported in reference 5. The flap was arranged for locking at downward, or positive, flap deflections from 0° to 60° in 10° increments.

The model was fitted with a single chordwise row of pressure orifices 21 inches from one end of the airfoil and located along the chord as shown in table II and figure 1. Tubes leading from these orifices were brought out through one end of the wing (fig. 2) and connected to a multiple-tube manometer that records photographically.

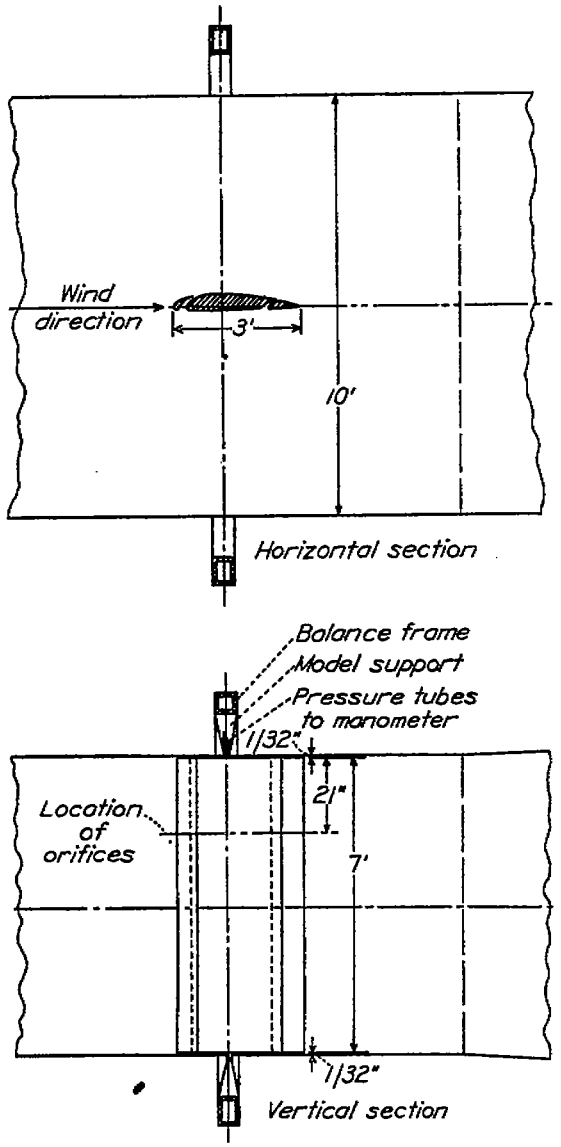

FIGURE 2.—Model installation for two-dimensional flow tests in the 7- by 10-foot wind tunnel.

TEST INSTALLATION

The model was mounted in the closed test section of the NACA 7- by 10-foot wind tunnel (reference 5). Because the model completely spanned the tunnel except for small clearances at each end (fig. 2), approximately two-dimensional flow was obtained. Torque tubes attached to the balance frame held the model rigid and also served as conduits for the pressure tubes. The angle of attack was set from outside the tunnel by rotating the torque tubes with a calibrated electric drive.

TESTS

The tests, except for those at large angles of attack in which the dynamic pressure was lowered as much as 19 percent, were run at an average dynamic pressure of 16.37 pounds per square foot. The decrease in dynamic pressure was necessary to measure the peak pressures because of limitations in the manometer. The average dynamic pressure, 16.37 pounds per square foot, corresponds to a tunnel velocity of 80 miles per hour and a test Reynolds number, based on the chord of the airfoil with flap retracted, of 2,190,000. Because of the turbulence in the air stream, the effective Reynolds number was 3,500,000. (See reference 6.)

The model was tested with the slotted flap deflected from 0° to 60° in 10° increments. Tests were made at each flap deflection through an angle-of-attack range from about zero lift to approximately maximum lift in 4° increments. With the model at a given angle of attack and flap setting, time was allowed for the tunnel and for the manometer to become stable before the pressures were recorded.

PRESENTATION OF DATA

PRESSURE DIAGRAMS

All the diagrams of pressures over the upper and lower surfaces of the airfoil-slot-flap combination are given as pressure coefficients P
where

$$P=\frac{p-p_0}{q}$$

and

p static pressure at a point on airfoil
p_0 static pressure in free air stream
q dynamic pressure of free air stream

Pressures over the airfoil with the fixed slot are shown in figure 3 and pressures over the airfoil with the fixed slot and the slotted flap are shown in figures 4 to 10. A comparison of the loads on the plain airfoil with the loads on the slotted airfoil is shown in figure 11, and a comparison of the loads on the plain airfoil with slotted flap with the loads on the slotted airfoil with slotted flap is shown in figure 12.

In figures 3 to 10 the pressures over the main airfoil and the slat are plotted normal to the airfoil chord and the pressures over the slotted flap are plotted normal to the undeflected flap chord line. In order to prevent overlapping of the component parts of the combination and to keep the curves as large as possible, the slat was moved forward and the flap was moved rearward from the normal positions. The pressures are plotted for the component parts in the positions shown by solid lines. The normal positions of the slat and the flap are shown by dashed lines. The pressures over the main airfoil and the slat for figures 11 and 12 are

plotted normal to the airfoil chord, and the pressures over the slotted flap are plotted normal to the deflected flap chord line. The position of the component parts in these figures is normal.

COEFFICIENTS

The pressure diagrams were mechanically integrated to obtain data from which standard nondimensional section coefficients were computed. Where the term "flap alone" or "slat alone" is used, it refers to the forces and the moments on the flap or the slat in the presence of the rest of the airfoil-slot-flap combination. The section coefficients are defined as follows:

c_n normal-force coefficient of slotted airfoil with flap (n/qc)

c_{n_f} normal-force coefficient of flap alone (n_f/qc_f)

c_{n_s} normal-force coefficient of slat alone (n_s/qc_s)

c_{c_s} chord-force coefficient of slat alone (x_s/qc_s)

c_{r_s} resultant-force coefficient of slat alone $\left(\sqrt{c_{n_s}^2+c_{c_s}^2}\right)$

c_m pitching-moment coefficient of slotted airfoil with flap about quarter-chord point of airfoil (m/qc^2)

c_{m_f} pitching-moment coefficient of flap alone about quarter-chord point of flap (m_f/qc_f^2)

$c_{m_{s_n}}$ pitching-moment coefficient of normal force of slat alone about leading edge of slat (m_{s_n}/qc_s^2)

$c_{m_{s_c}}$ pitching-moment coefficient of chord force of slat alone about leading edge of slat (m_{s_c}/qc_s^2)

c_{m_s} pitching-moment coefficient of slat alone about leading edge of slat $\left(c_{m_{s_c}}+c_{m_{s_n}}\right)$

$(c.p.)$ center-of-pressure location of slotted airfoil with flap in percent airfoil chord from leading edge of airfoil $\left[\left(0.25-\frac{c_m}{c_n}\right)\times 100\right]$

$(c.p.)_f$ center-of-pressure location of flap alone in percent flap chord from leading edge of flap $\left[\left(0.25-\frac{c_{m_f}}{c_{n_f}}\right)\times 100\right]$

$(c.p.)_{s_n}$ center-of-pressure location of slat alone in percent slat chord from leading edge of slat $\left(-\frac{c_{m_{s_n}}}{c_{n_s}}\times 100\right)$

$(c.p.)_{s_c}$ center-of-pressure location of slat alone in percent slat chord above chord line of slat $\left(\frac{c_{m_{s_c}}}{c_{c_s}}\times 100\right)$

where

n normal force on slotted airfoil with flap

n_f normal force on flap alone normal to chord of flap

n_s normal force on slat alone

x_s chord force on slat alone

m pitching moment of slotted airfoil with flap

m_f pitching moment of flap alone

m_{s_n} pitching moment of slat alone about leading edge of slat, due to normal force

m_{s_c} pitching moment of slat alone about chord line of slat, due to chord force

c chord of airfoil with flap neutral

c_f chord of slotted flap (over-all length of flap)

c_s chord of slat (projected distance along airfoil chord line) (See fig. 1.)

and

α_0 angle of attack for infinite aspect ratio

δ_f angle of flap deflection

With the exception of the chord-force moment of the slat, the coefficients for the combination were derived from the normal forces alone, the chord force of the flap being neglected. Neglecting the normal-force component of the chord force on the flap in calculations for the combination reduced the normal-force coefficients by a maximum of approximately 0.08. Because the skin friction of the flap will enter into any correction for this discrepancy, no attempt was made to include a correction for flap-chord force in the final results. Inasmuch as the model completely spanned the jet, the integrated results, which are in coefficient form, may be used as section characteristics.

Figures 13 to 16 show the section characteristics of the combination, of the slat alone, and of the flap alone. Figure 15 shows a vectorial representation of the resultant-force coefficient on the slat alone.

PRECISION

Experimental errors in the results presented in this report are believed to be within the following limits:

p	±2 percent
q	±1 percent
α_0	±0.1°
δ_f	±0.5°

The normal-force coefficient of the combination was corrected as explained in reference 5. This correction tends to reduce the magnitudes of the pressures; the results for the slat and the flap, which are uncorrected, should be conservative.

DISCUSSION

SECTION PRESSURE DISTRIBUTION

The pressure curves (figs. 3 to 10) show the distribution of pressure over the upper and lower surfaces of the airfoil for various combinations. These curves may be used for designing of ribs, slats, and flaps as well as for showing the change in distribution as the flap is deflected. In general, these curves show that the fixed slot has little effect on the net pressure distribution except that it maintains flow above the stall range for the plain wing.

705859 O - 46 - 7

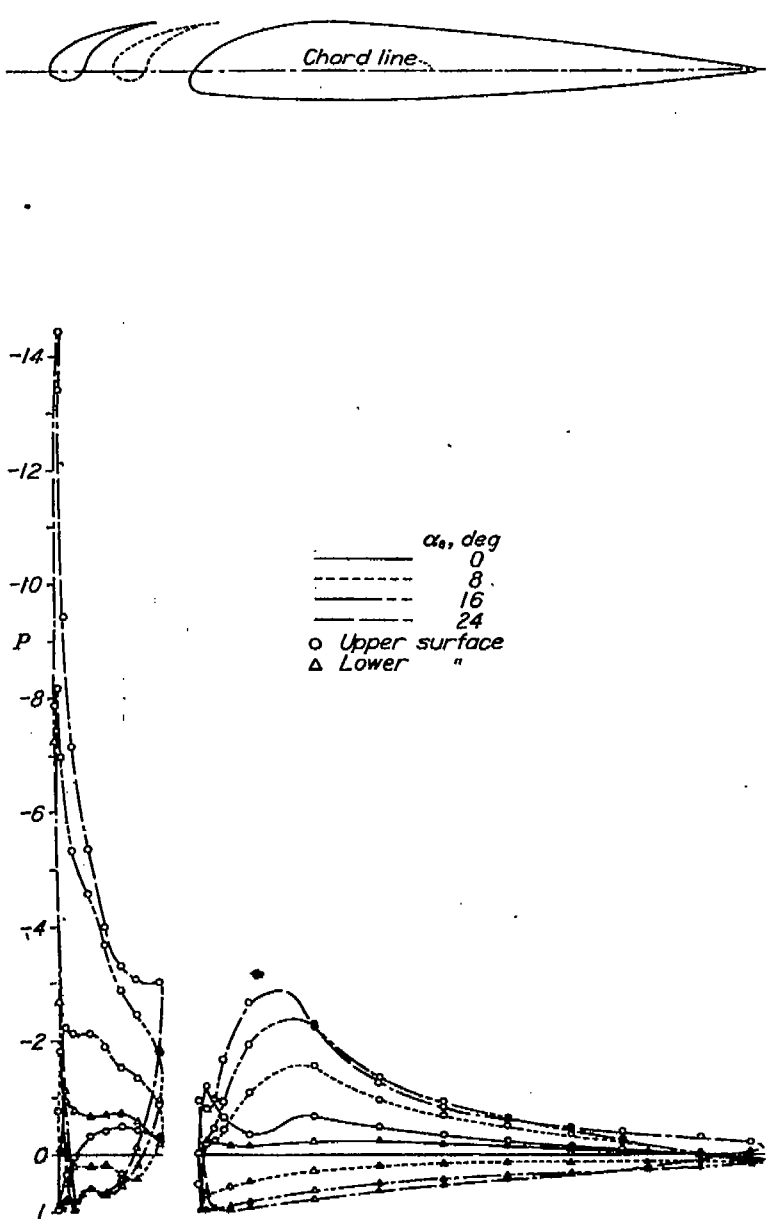

FIGURE 3.—Pressure distribution on the NACA 23012 airfoil with the fixed slot at various angles of attack.

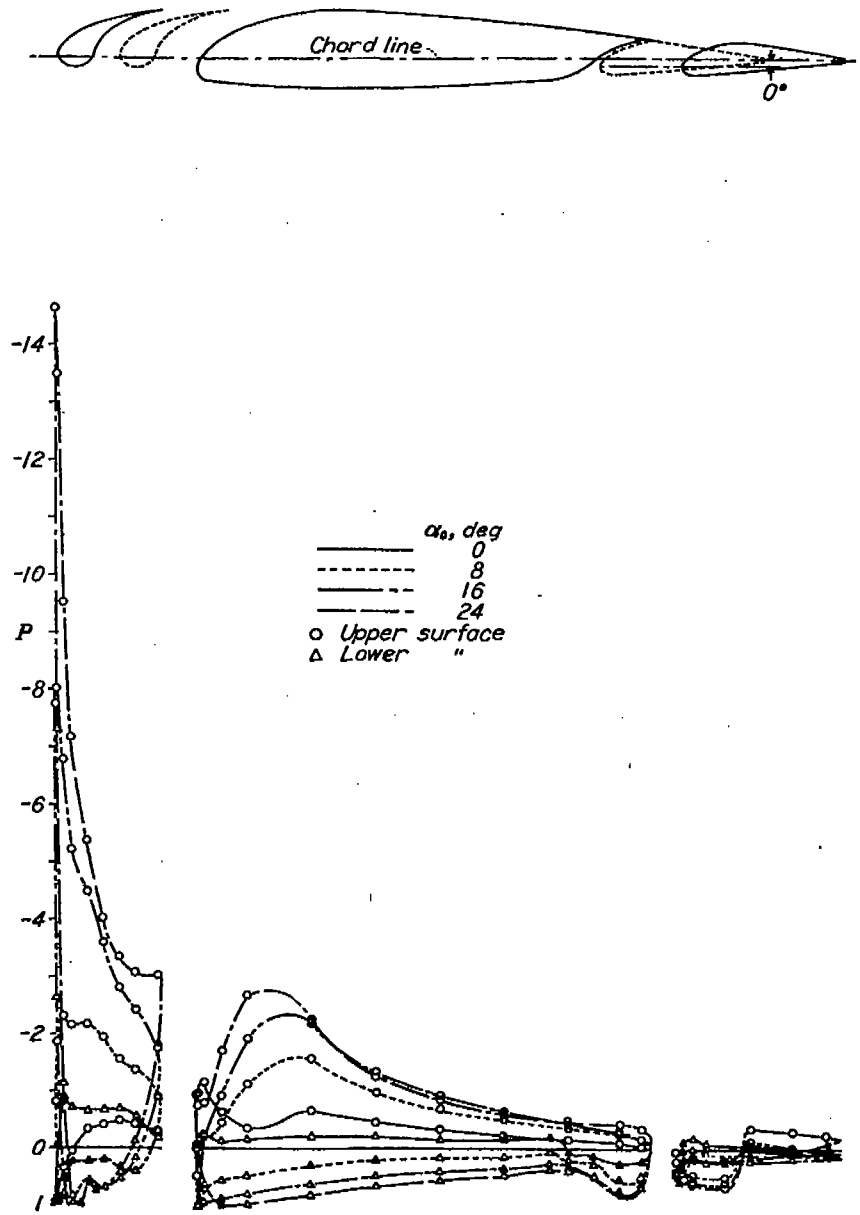

FIGURE 4.—Pressure distribution on the NACA 23012 airfoil with the fixed slot and 0.266c slotted flap at various angles of attack. Flap deflection, 0°.

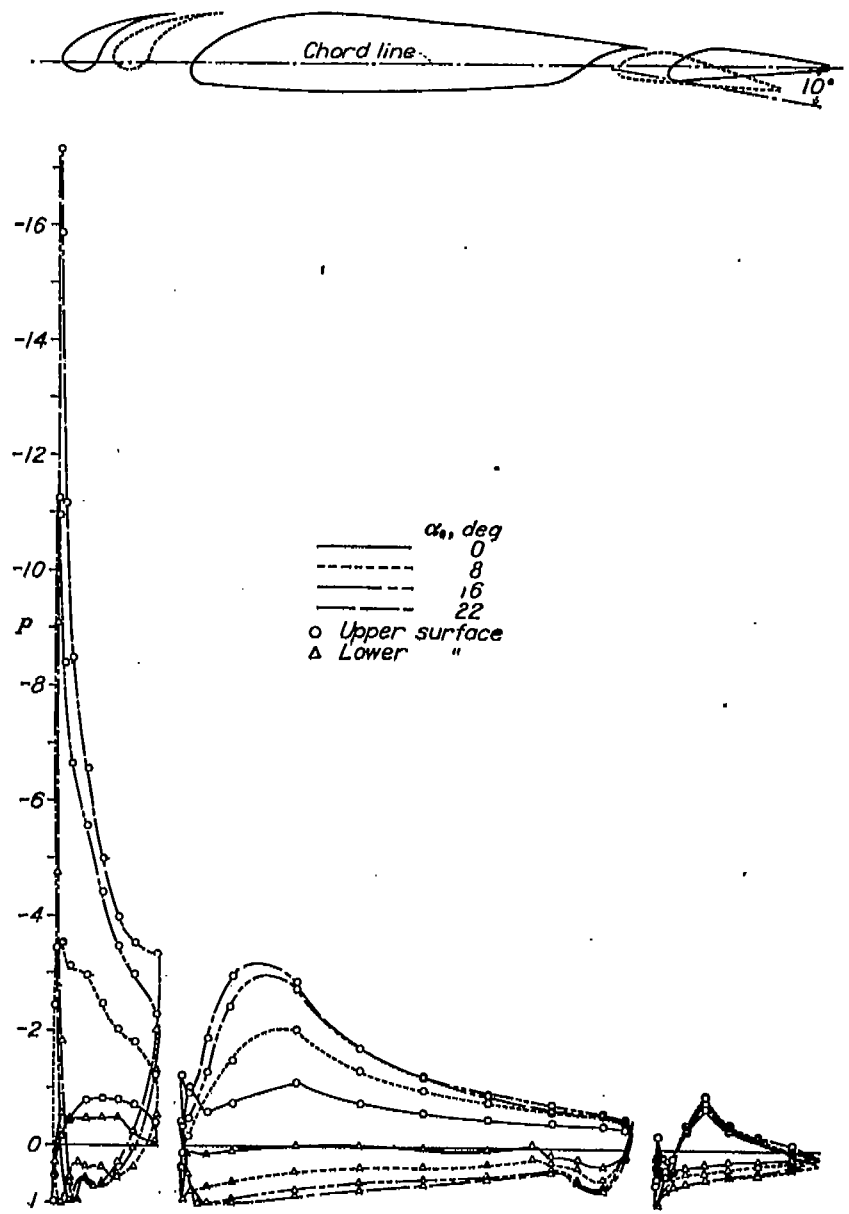

FIGURE 5.—Pressure distribution on the NACA 23012 airfoil with the fixed slot and 0.2566c slotted flap at various angles of attack. Flap deflection, 10°.

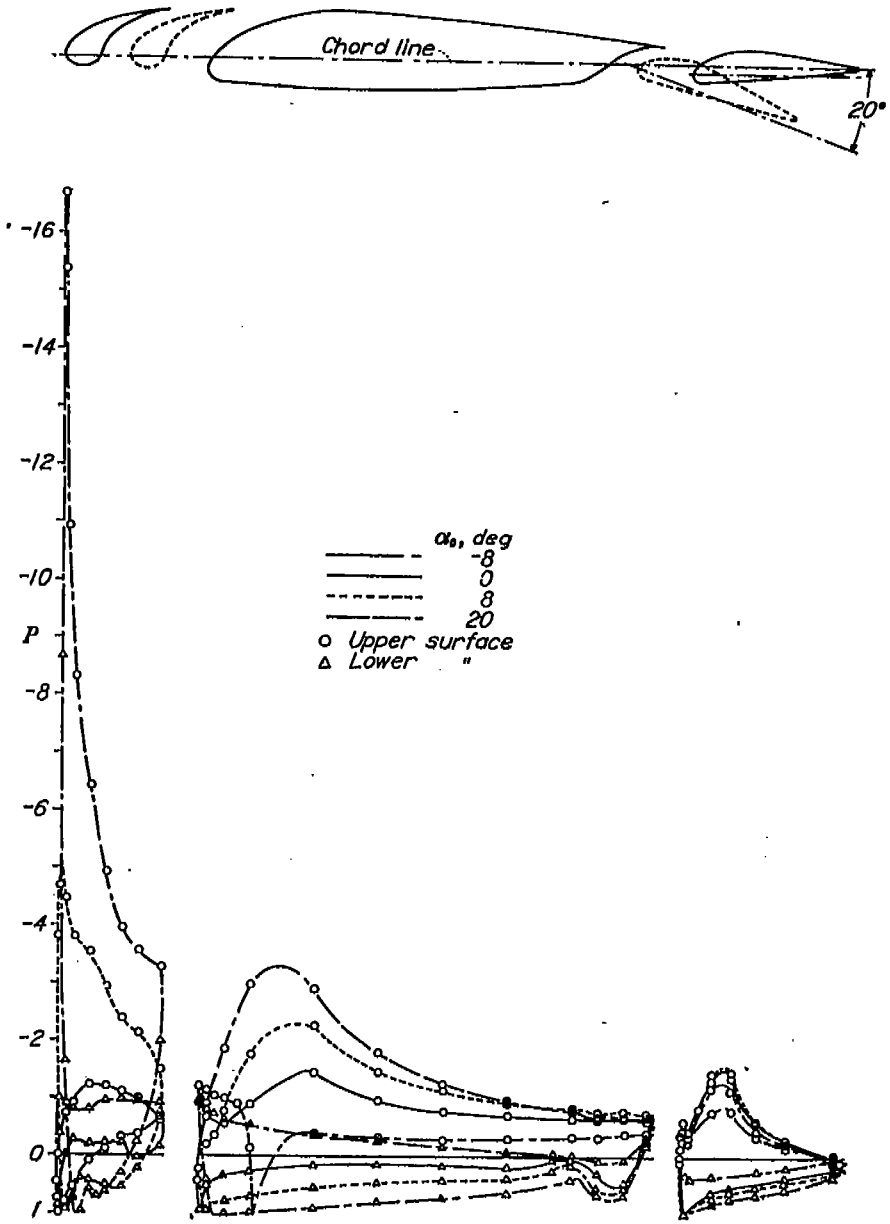

FIGURE 6.—Pressure distribution on the NACA 23012 airfoil with the fixed slot and 0.2566c slotted flap at various angles of attack. Flap deflection, 20°.

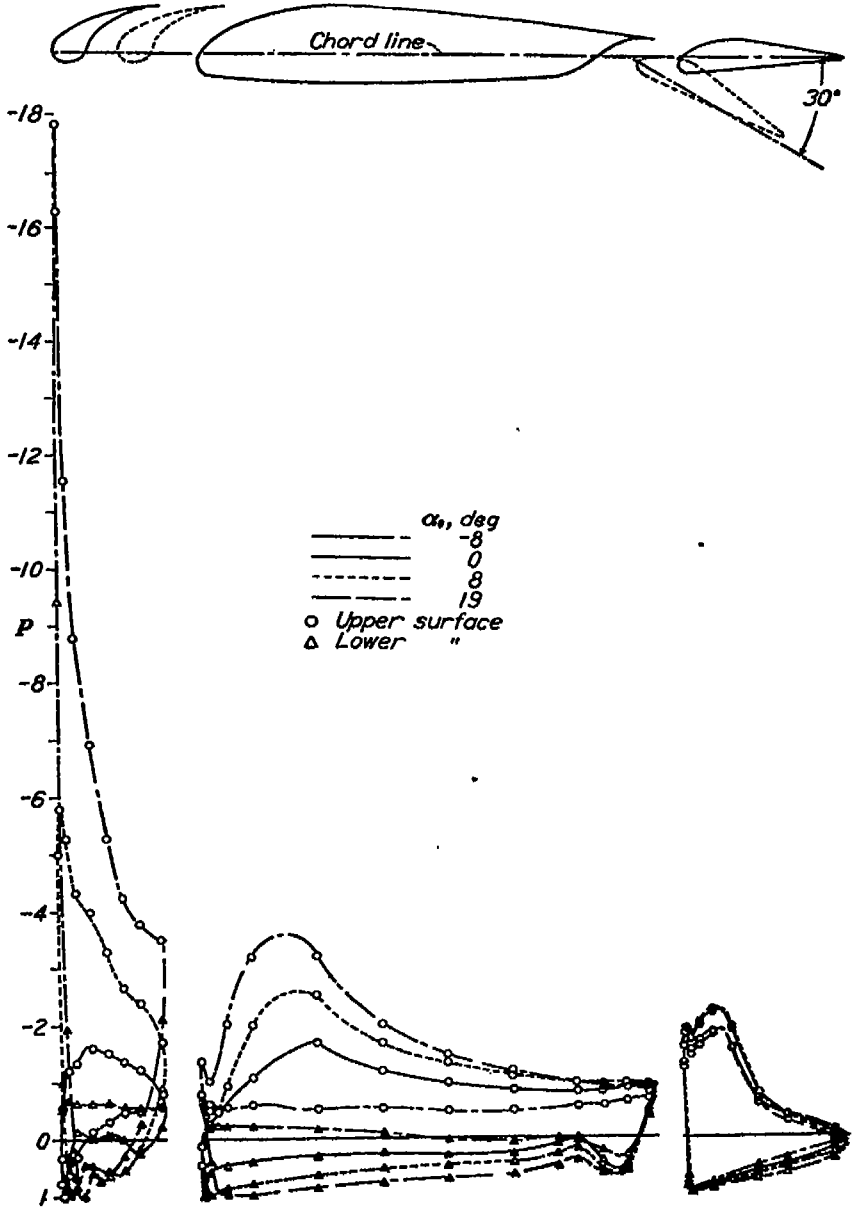

FIGURE 7.—Pressure distribution on the NACA 23012 airfoil with the fixed slot and 0.25$\overline{66}c$ slotted flap at various angles of attack. Flap deflection, 30°.

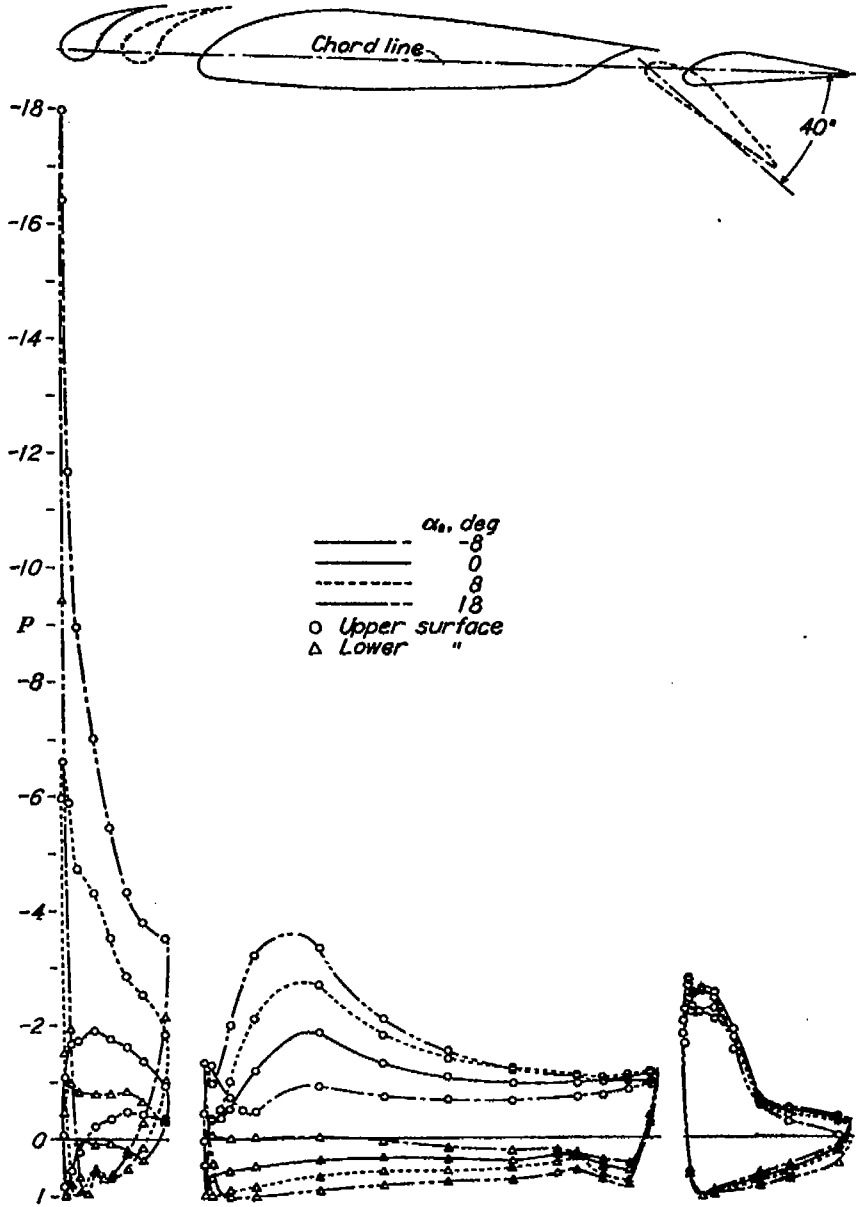

FIGURE 8.—Pressure distribution on the NACA 23012 airfoil with the fixed slot and 0.25$\overline{66}c$ slotted flap at various angles of attack. Flap deflection, 40°.

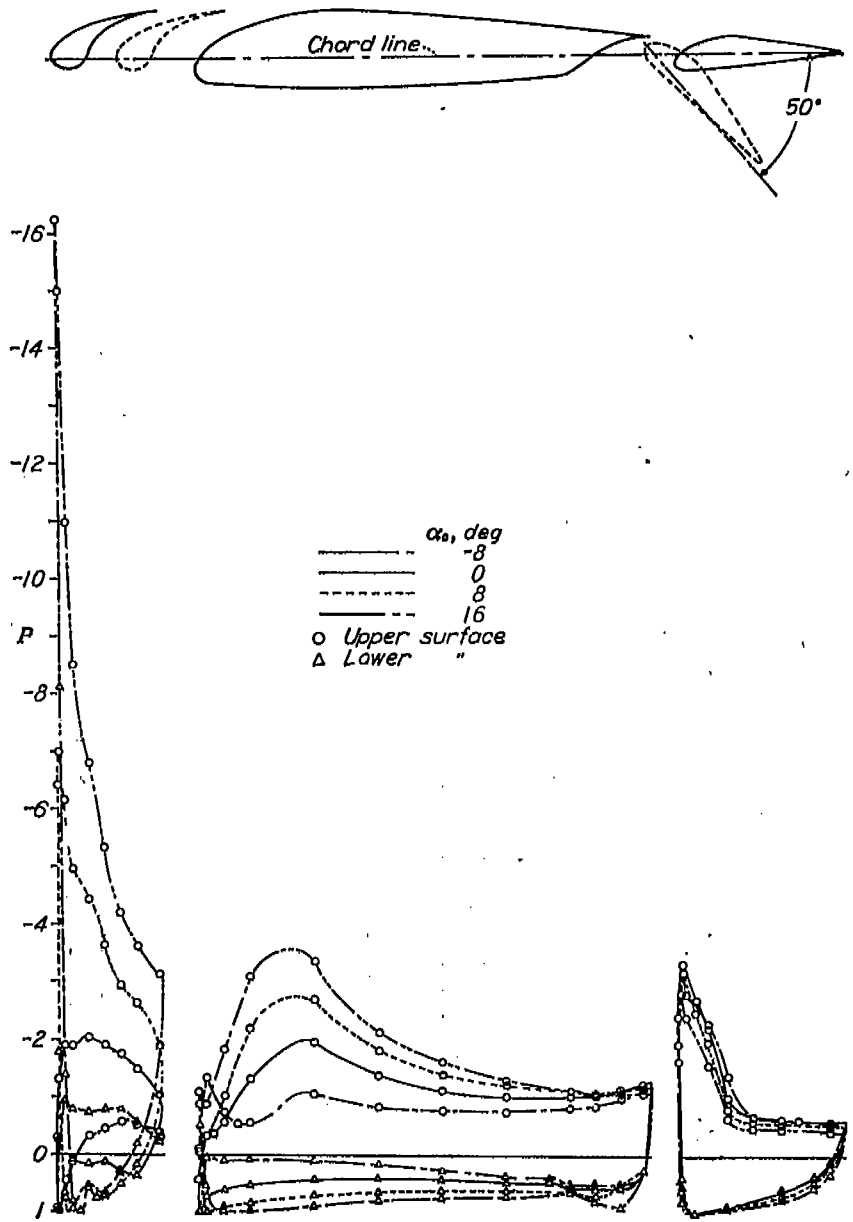

FIGURE 9.—Pressure distribution on the NACA 23012 airfoil with the fixed slot and 0.256c slotted flap at various angles of attack. Flap deflection, 50°.

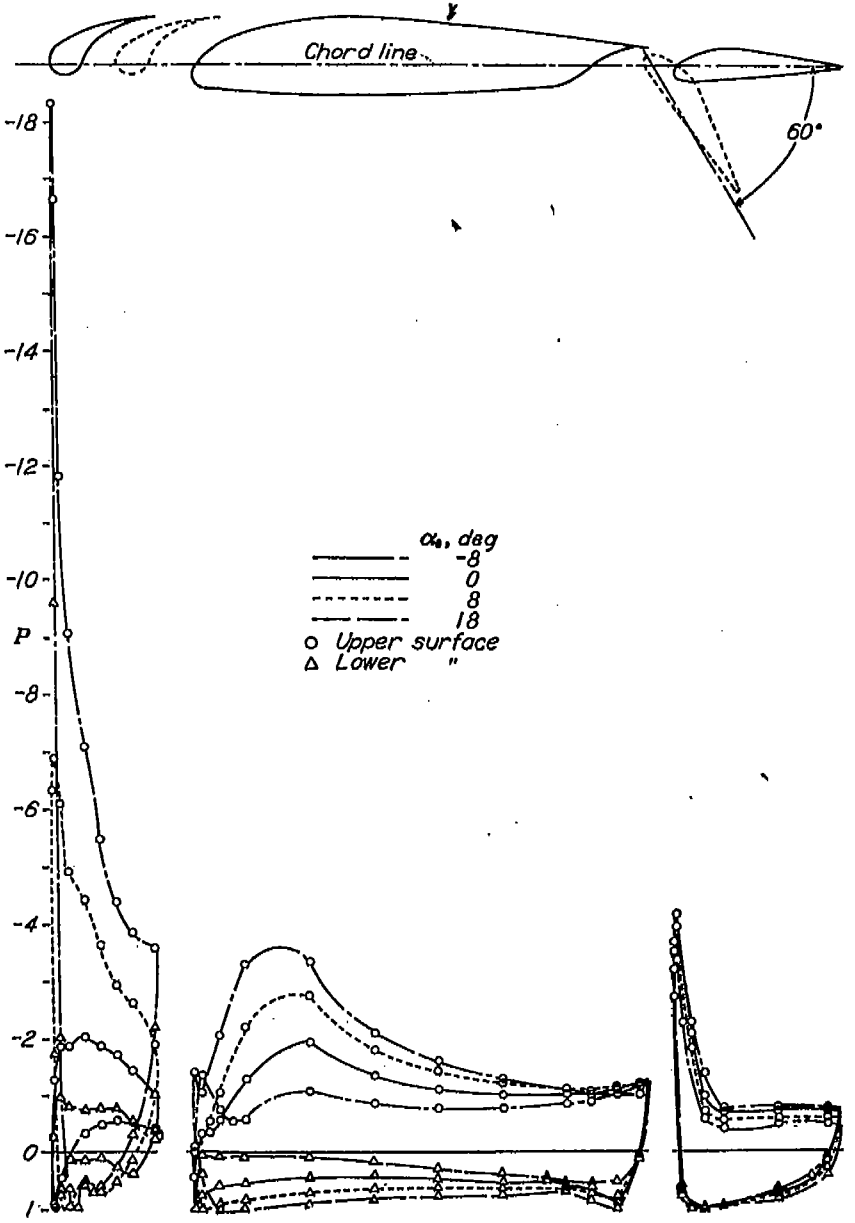

FIGURE 10.—Pressure distribution on the NACA 23012 airfoil with the fixed slot and 0.256c slotted flap at various angles of attack. Flap deflection, 60°.

The shapes of the pressure curves for the model with the slotted flap deflected (figs. 4 to 10) are generally very similar to those of the curves for the slotted flap deflected on a plain NACA 23012 airfoil (reference 7); this similarity shows that the flaps have the same characteristics as to extent of peak pressure, occurrence

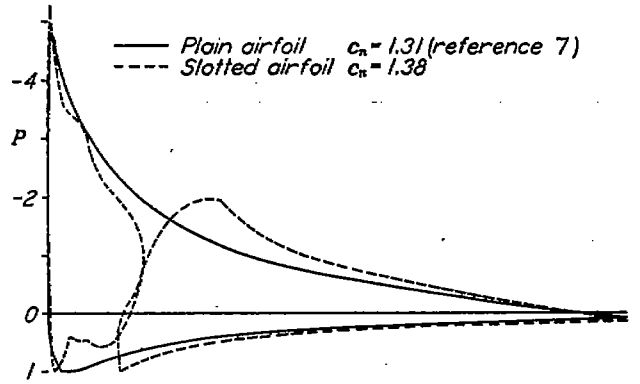

FIGURE 11.—Comparison of the pressure distribution on the NACA 23012 airfoil with a fixed slot with that on a plain NACA 23012 airfoil. α_a=12°.

of double peak pressures, and magnitude of peak negative pressures. No chord-force diagrams were included in this report because of the similarity of pressures on the slotted flap in this investigation to pressures on the slotted flap reported in reference 7 and because such diagrams can be constructed from normal-force diagrams.

The pressure curves for the fixed slat (figs. 3 to 10) are similar in general shape to the curves shown in references 2 and 4, but the maximum peak negative pressures are much higher on the fixed slat than they were on the Handley Page type of slat. The extremely high negative pressures ($P=-18$) at the nose of the slat might be very detrimental at relatively high airplane speeds because of compressibility effects. A careful inspection of the pressure curves will show that the location of the extremely high negative values of P is very critical. It is quite possible, therefore, that in the previous investigations of Handley Page slots the pressure orifices were so located that they inadvertently missed these high negative pressures. Diagrams show that the pressure variation over the lower surface of the slat is similar to the pressure variation over the lower surface of the main airfoil at the slot entry for the slotted flap.

The pressure diagrams for the center portion of the airfoil (figs. 3 to 10) show a similarity to the pressure diagrams for a slotted flap.

The similarity of flow about the main portion of the airfoil for several airfoil-flap arrangements (reference 8) indicates that the forces on the fixed slat in combination with any of the flaps would have approximately the same pressure curve as to magnitude of pressures and general shape. Because the addition of the fixed slot had little effect on the pressures on the slotted flap, it is reasonable to assume that the pressures on other flaps would be only slightly changed. It is to be remembered that the forces on the slat would change with any alteration in shape of slat or slot.

A comparison of the pressures over the plain airfoil with pressures over the slotted airfoil at the same angle of attack (fig. 11) and a comparison of the pressures over the plain airfoil with slotted flap with the pressures over the slotted airfoil with slotted flap at the same angle of attack (fig. 12) show the following: The plain and slotted combinations both carry about the same load. The addition of the slot does not change peak nose pressure to any extent. The center portion of the slotted airfoil carries more load and the slat carries less load than a proportional section of plain airfoil. The load on the flap is slightly increased by the addition of a slot.

The main effect of the fixed slot on the plain airfoil with slotted flap is to increase the angle of attack for the stall. The continuation of flow about the airfoil at high angles of attack accounts for the extremely high values of P obtained.

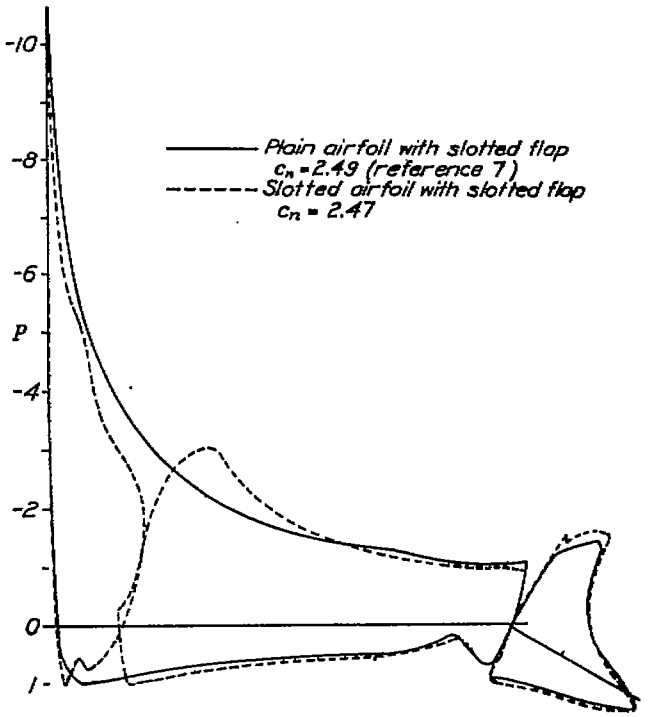

FIGURE 12.—Comparison of the pressure distribution on the NACA 23012 airfoil with a fixed slot and a 0.2566c slotted flap with that on a plain NACA 23012 airfoil with 0.2566c slotted flap. Flap deflection, 30°; α_a=12°.

AERODYNAMIC SECTION CHARACTERISTICS

A comparison of the section characteristics for the combination (fig. 13) with results reported in references 1 and 7 shows the following: The normal-force coefficients for the combination agree very well with the force-test results of reference 1; the pitching-moment coefficients for the arrangement tested show an increase over the coefficients for the plain airfoil with

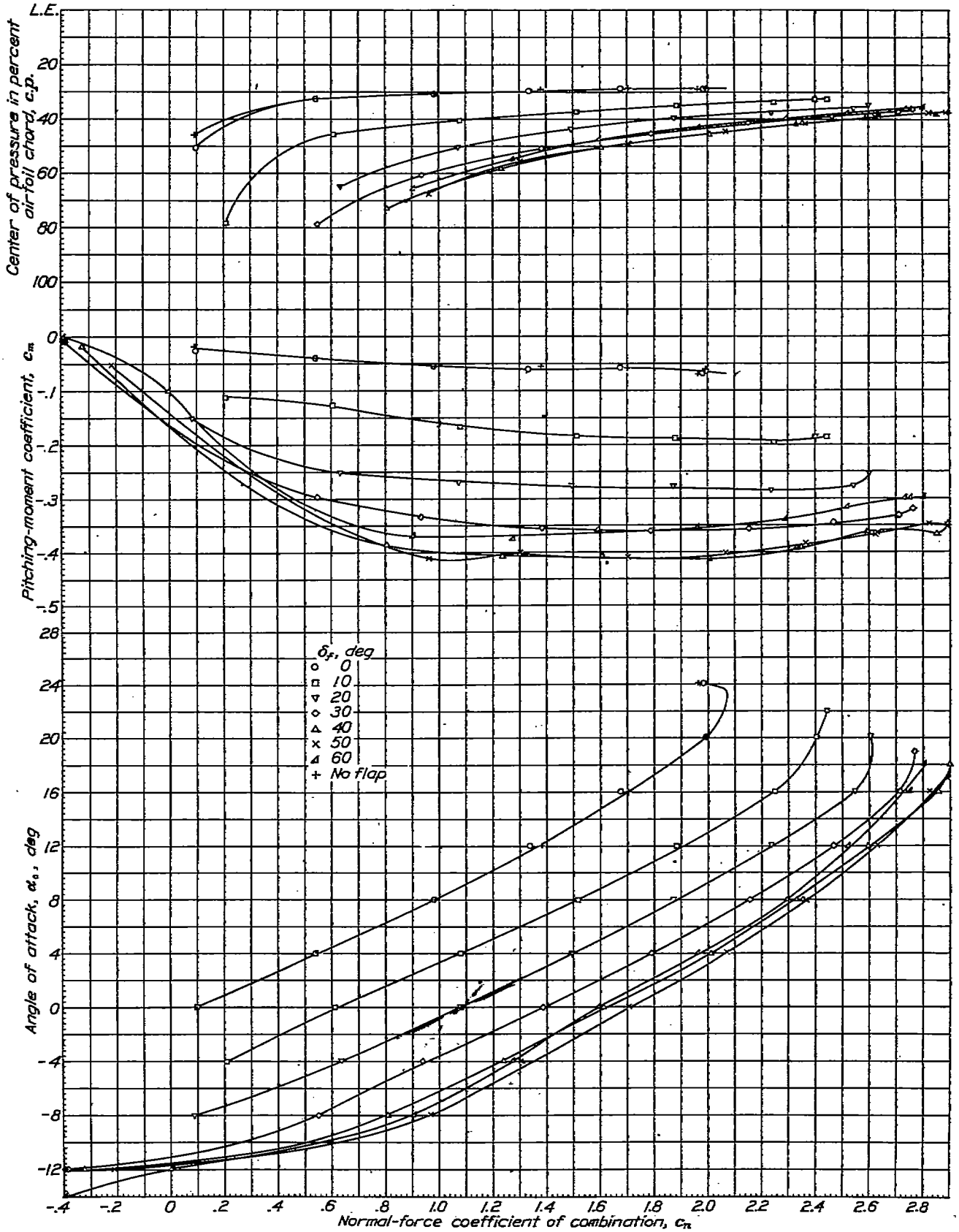

FIGURE 13.—Section characteristics of the NACA 23012 airfoil with the fixed slot and 0.2566c slotted flap.

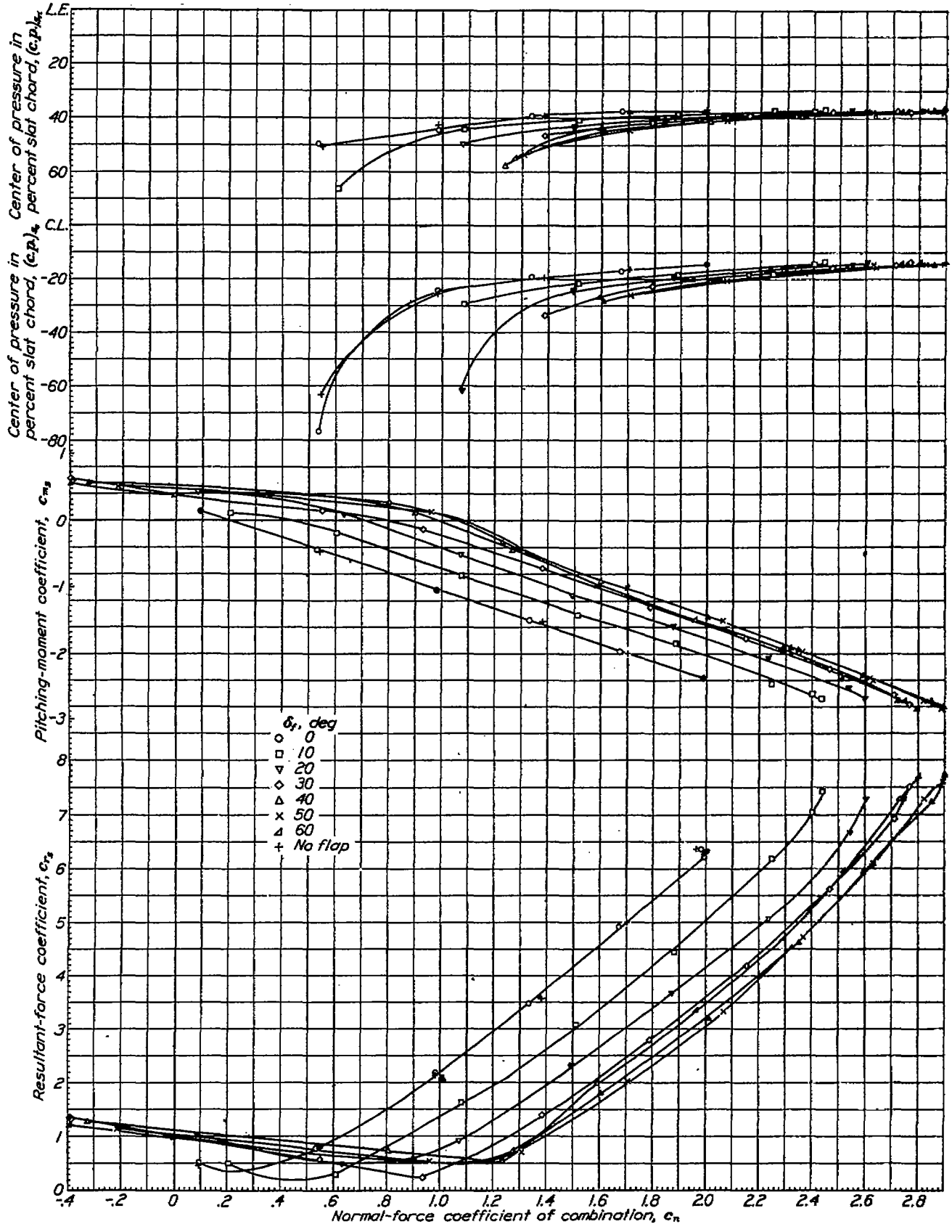

FIGURE 14.—Section characteristics of the 0.1650c slat on the NACA 23012 airfoil with 0.2566c slotted flap.

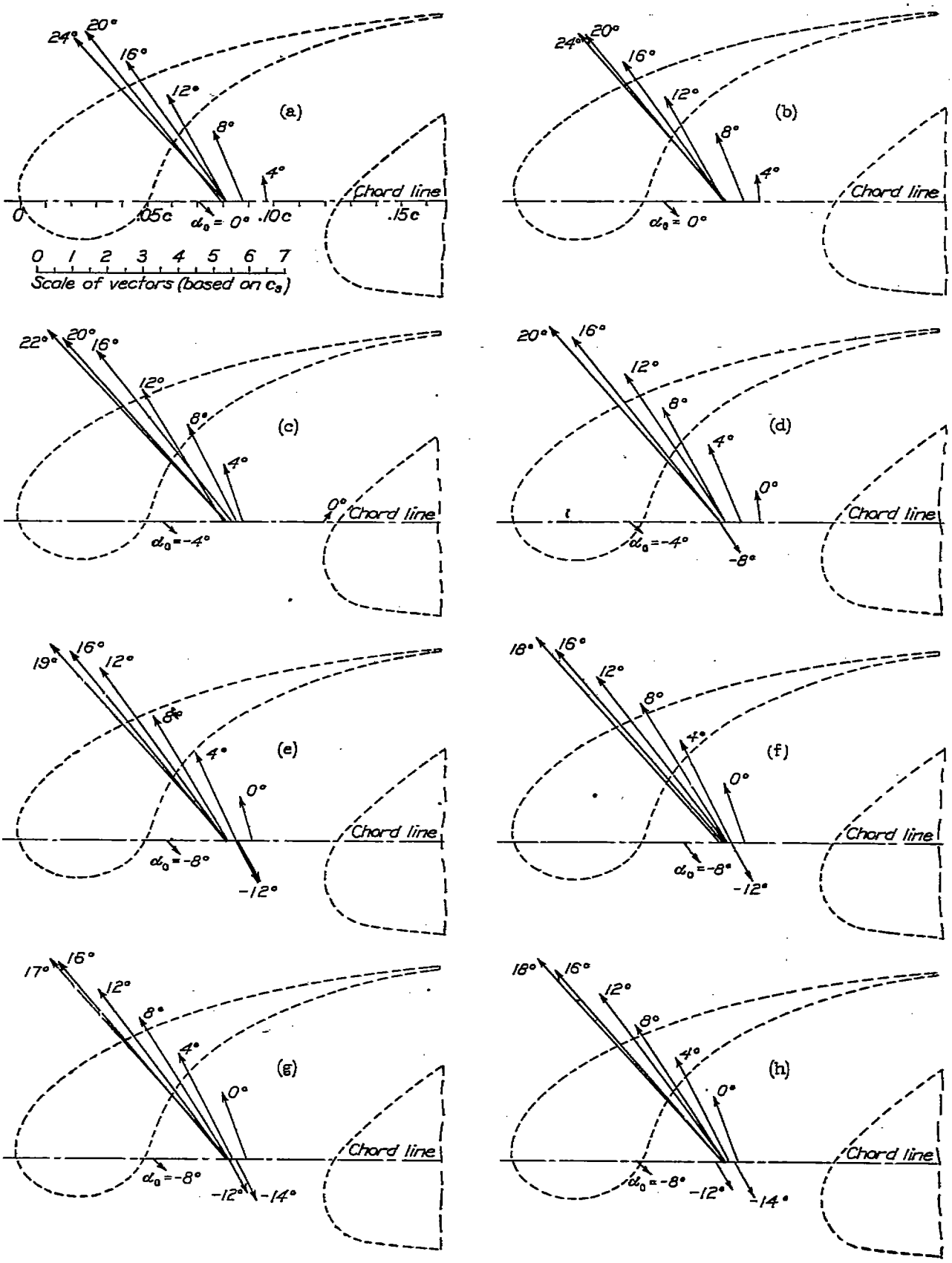

(a) No flap.
(b) $\delta_f = 0°$.
(c) $\delta_f = 10°$.
(d) $\delta_f = 20°$.
(e) $\delta_f = 30°$.
(f) $\delta_f = 40°$.
(g) $\delta_f = 50°$.
(h) $\delta_f = 60°$.

FIGURE 15.—Vectorial representation of resultant-force coefficient of the 0.1650c slat on the NACA 23012 airfoil with the 0.2565c slotted flap.

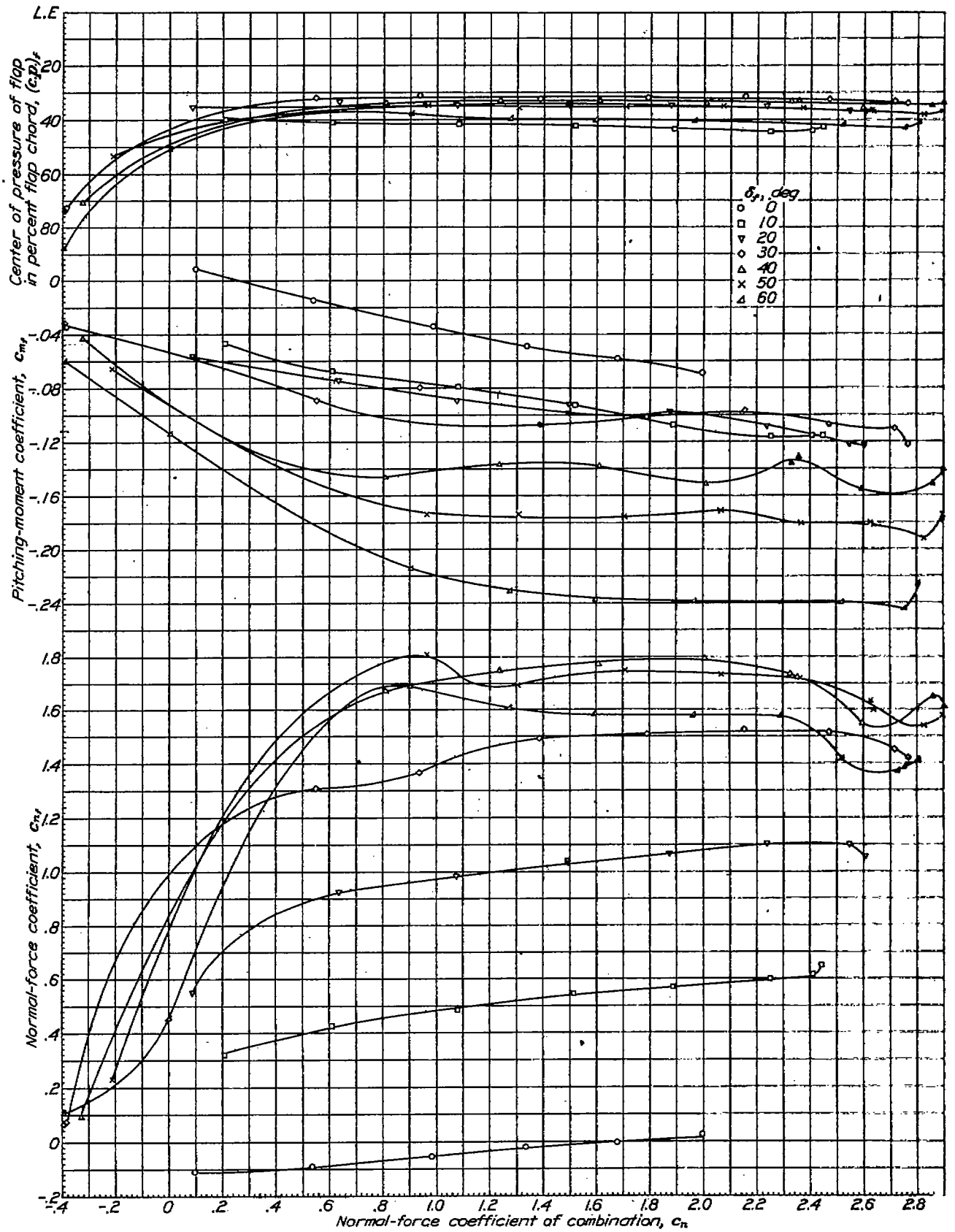

FIGURE 16.—Section characteristics of the 0.256c slotted flap on the NACA 23012 airfoil with the fixed slot.

slotted flap (reference 7); and because the normal-force coefficients remain approximately the same on both airfoils for a given angle of attack, the center of pressure moves rearward. No quantitative comparison of pitching-moment coefficients with force-test results is made because the chord forces of flap and airfoil have been neglected in this report; however, the values of c_m obtained by the two methods show reasonable agreement. The angle of attack for the stall is slightly lower for the pressure-distribution tests, but no effort was made to obtain absolute values because the same arrangement had been reported in reference 1.

Figures 14 and 15 show the section characteristics of the slat alone. The resultant-force coefficient for the slat tested is much higher than that reported for the Handley Page slat (references 2 and 4). The forces, however, act in the same direction and from approximately the same point. The maximum resultant force acts forward along a line that makes an angle of approximately 47° with the chord line and intersects it at the 0.40 c_s point. Figure 15 should be useful in the design of slat supports.

A comparison of the section characteristics of the flap alone (fig. 16) shows that the loads on the flap build up more slowly than do the loads on the combination, except in the normal-force-coefficient range below 1 with flap deflections greater than 30°. A comparison of the section characteristics of the flap alone on the slotted airfoil (fig. 16) with the section characteristics of the flap alone on a plain airfoil (reference 7) shows the flap loads and moments to be little affected by the addition of the leading-edge slot. Inasmuch as the loads on the flap in combination with a slotted airfoil are approximately the same as the loads on the flap in combination with a plain airfoil, no chord-force coefficients are given. The chord-force coefficients reported in reference 7 should be applicable.

CONCLUSIONS

The peak pressures at the nose of the slat were very high in the range of angle of attack where slots are useful.

The forces on the slat were smaller than the forces on the same portion of a plain airfoil at low angles of attack but built up to very high values above the stall of the plain airfoil. These forces were much higher than previously published loads on Handley Page slats.

The loads on the flap on the slotted airfoil were approximately the same as the loads on a flap on a plain airfoil; therefore, any conventional flap should show little change in load if a similar leading-edge slot were added to the combination.

LANGLEY MEMORIAL AERONAUTICAL LABORATORY,
NATIONAL ADVISORY COMMITTEE FOR AERONAUTICS,
LANGLEY FIELD, VA., *July 30, 1941.*

REFERENCES

1. Bamber, M. J.: Wind-Tunnel Tests of Several Forms of Fixed Wing Slot in Combination with a Slotted Flap on an N. A. C. A. 23012 Airfoil. T. N. No. 702, NACA, 1939.
2. Jacobs, Eastman N.: Pressure Distribution on a Slotted R. A. F. 31 Airfoil in the Variable Density Wind Tunnel. T. N. No. 308, NACA, 1929.
3. Gauvain, William E.: Wind-Tunnel Tests of a Clark Y Wing with "Maxwell" Leading-Edge Slots. T. N. No. 598, NACA, 1937.
4. Ormerod, A.: Slotted R. A. F. 34 Bristol Fighter.—Measurement of Forces on Slat in Flight. R. & M. No. 1477, British A. R. C., 1932.
5. Wenzinger, Carl J., and Harris, Thomas A.: Wind-Tunnel Investigation of an N. A. C. A. 23012 Airfoil with Various Arrangements of Slotted Flaps. Rep. No. 664, NACA, 1939.
6. Pinkerton, Robert M.: The Variation with Reynolds Number of Pressure Distribution over an Airfoil Section. Rep. No. 613, NACA, 1938.
7. Wenzinger, Carl J., and Delano, James B.: Pressure Distribution over an N. A. C. A. 23012 Airfoil with a Slotted and a Plain Flap. Rep. No. 633, NACA, 1938.
8. Wenzinger, Carl J., and Rogallo, Francis M.: Résumé of Air-Load Data on Slats and Flaps. T. N. No. 690, NACA, 1939.

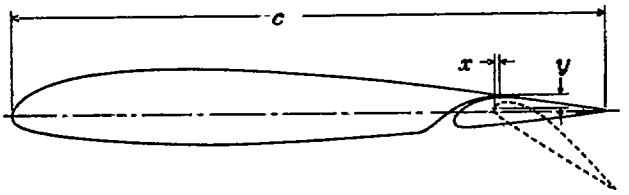

TABLE I.—ORDINATES FOR AIRFOIL AND SLOTTED FLAP AND PATH OF FLAP NOSE

[All dimensions in percent of wing chord]

NACA 23012 AIRFOIL

Station	Upper surface	Lower surface
0	------	0
1.25	2.67	−1.23
2.5	3.61	−1.71
5.0	4.91	−2.26
7.5	5.80	−2.61
10	6.48	−2.92
15	7.19	−3.50
20	7.50	−3.97
25	7.60	−4.28
30	7.55	−4.46
40	7.14	−4.48
50	6.41	−4.17
60	5.47	−3.67
70	4.36	−3.00
80	3.08	−2.16
90	1.66	−1.23
95	.92	−.70
100	.13	−.13
Leading-edge radius: 1.58 slope of radius through end of chord: 0.306.		

SLOTTED FLAP

Station	Upper surface	Lower surface
0	−1.29	−1.29
.40	−.32	−2.05
.72	.04	−2.21
1.36	.61	−2.36
2.00	1.04	−2.41
2.64	1.40	−2.41
3.92	1.94	------
5.20	2.30	------
5.66	------	−2.16
6.48	2.53	------
7.76	2.63	------
9.03	2.58	------
10.31	2.46	------
15.66	1.68	−1.23
20.66	.92	−.70
25.66	.13	−.13
Center of leading-edge arc: 0.91	−1.29	------
Leading-edge radius: 0.91		

PATH OF FLAP NOSE

δ_f (deg)	x	y
0	8.36	3.91
10	5.41	3.63
20	3.53	3.45
30	2.63	3.37
40	1.35	2.43
50	.50	1.63
60	.12	1.48

CONTOUR OF SLOT

Station	Ordinate
72.32	−1.02
74.57	.67
76.32	1.76
77.82	2.30
79.32	2.65
80.82	2.82
82.70	2.64

Arc center		Arc radius
66.65	4.67	7.97

TABLE II.—ORIFICE LOCATIONS ON AIRFOIL-SLOT-FLAP COMBINATION TESTED

[Orifice locations on upper and lower surfaces in percent airfoil chord from leading edge of airfoil]

Fixed slat	
Orifice	Location
0	0
1	.25
2	1.25
3	2.50
4	[a] 3.75
5	5.00
6	[a] 6.25
7	7.50
8	10.00
9	12.50
10	16.00

Airfoil	
Orifice	Location
0	12.00
1	12.25
2	13.25
3	14.50
4	[b] 16.00
5	[a] 17.00
6	[b] 18.00
7	20.00
8	30.00
9	40.00
10	50.00
11	60.00
12	67.00
13	70.00
14	74.00
15	78.00
16	81.50

Slotted flap	
Orifice	Location
0	74.34
1	74.66
2	74.96
3	75.62
4	76.91
5	78.96
6	82.04
7	85.89
8	90.38
9	92.95
10	95.51
11	98.08

[a] Lower surface only.
[b] Upper surface only.